

Antibody-Based Proteomics Analysis of Tumor Cell Signaling Pathways

Steven Pelech and Hong Zhang

Introduction

The promise of personalized medicine is ultimately contingent on the successful identification of specific biomarkers for diseases and therapeutic modalities that can compensate for the molecular lesions that underlie these diseases. In the case of cancer, more than two decades of research have demonstrated the critical roles of a relatively small subset of proteins that are encoded by oncogenes and tumor suppressor genes. The gain of function of perhaps just a few oncoproteins and the loss of function of only a small number of tumor suppressor proteins in the right combinations may culminate in full neoplastic transformation. However, there may well be billions of such genetic change combinations so that every cancer patient has a unique form of the disease. Presently, just under half of cancer patients die from their disease within 5 years so there is a pressing need for development of new diagnostics and treatments.

Like many chronic diseases associated with aging, cancer is a systems disorder. Most of the known oncogenes and tumor suppressor genes specify protein kinases, their regulators or their target substrates. The human genome encodes at least 515 protein kinases (the kineome) (1,2) and 120 protein phosphatases (3), which catalyze the reversible phosphorylation of over a third of all proteins at more than 500,000 sites (the phosphoproteome) (4). Many of these phosphorylation events play key roles in the regulation of cell proliferation and survival. The phosphoproteome represents a relatively untapped source of potential biomarkers, and phosphoproteomics profiling should be extremely insightful for analysis of signaling pathways (5).

Our current knowledge of the composition and architecture of cell signaling systems is still extremely rudimentary. To elucidate these molecular communications webs, specific information is required concerning the spatial and temporal expression and activity of thousands of individual proteins in the nearly 200 different cell types in the organs and tissues of the human body. One of the major challenges of this decade will be the elucidation of these regulatory networks and the development of technologies to track their protein components in tumor biopsies and bodily fluids for cancer diagnostics.

While cancer is commonly viewed as a genetics disease, its successful treatment will require the knowledge of malfunctioning signal transduction at the protein level and the application of small molecule drugs. A very powerful arsenal of protein kinase inhibitors is being developed by the pharmaceutical industry, which is now spending about a third of their annual R&D budgets on this class of enzymes (6). We predict that within the next 10 years, most of the new drugs in clinical trials and entering the market place will be protein kinase inhibitors. One reason for this is because the industry is currently focused on only a few dozen of the protein kinases, and over 90% of them still remain to be explored for their therapeutic potential (4). Another impetus is that over 400 other

diseases have been linked to defective kinase signaling. Consequently, there will be an increasing demand to track signal transduction proteins in the near future.

Genomics verses Proteomics Profiling

All humans are at least 99.9% identical in their genomic sequences, whereas the genetic differences known as single nucleotide polymorphisms (SNP's) are thought to underpin our individual susceptibilities to disease and treatment. Thousands of in-born genetic errors leading to metabolic diseases have already been catalogued. So called "functional genomics" often refers to the expression of genes as revealed in measurement of the amount of mRNA transcripts that are produced from these genes. This is fairly easily achieved, because it is relatively simple to produce a specific DNA or oligonucleotide probe that features a nucleic acid sequence with bases that are fully complementary to the sequence of the target gene of interest. Such oligonucleotide probes can be created cheaply for pennies and rapidly within hours. These probes can be deployed in several different procedures, including Northern blotting analysis on gels, quantitative PCR's and gene microarrays. While gene microarrays are prone to less quantitative results with higher error rates, literally thousands of different mRNA's can be tracked on a single glass slide or silicon chip by this powerful technology. With the advent of gene microarrays, it has become feasible to track important SNP's and the expression of genes. Indeed, more than a US\$1 billion is expended annually on the application of gene microarrays in biomedical research. However at the end of the day, we are under the opinion that such analyses will have only limited value in the accurate diagnosis and treatment of cancer.

There are several reasons why we believe genomic profiling will prove to be inaccurate and potentially misleading. Firstly, while certain genetic mutations can be directly correlated with the loss or gain of function in their protein targets, it is not clear that these proteins may be actually responsible for the disease phenotype. The very nature of cell signaling networks with their high degree of redundancy and elaborate feedback systems probably means that most malfunctioning signal transduction proteins can be compensated for. Furthermore, the majority of altered gene transcriptions in diseased cells more likely arise from compensatory measures than those changes that are actually responsible for the disease state.

Secondly, it is well known that the correlation between mRNA and protein levels is quite poor, in the order of 50% for structural and metabolic pathway enzymes to much worse for signaling proteins (7). In some cases, the mRNA level of a protein may even decrease in response to a treatment, but the actual level of that protein can increase several-fold. For example, docetaxel treatment of head and neck squamous carcinoma cells has been reported to produce a 56% decrease in the mRNA level of the p19 cyclin-dependent kinase inhibitor protein, but the protein level of p19 was increased 30-fold as assessed with a specific antibody (8). Many mRNAs are not translated into proteins, and proteins often undergo different turnover rates than the mRNA for these proteins.

Thirdly, another limitation of indirect analysis of proteins by tracking their mRNA levels is that this provides no information about whether these proteins are subject to post-translation modifications. Although protein phosphorylation is the major means of post-transcriptional regulation, it is only one example of more than 20 possible types of regulatory covalent modifications of proteins. These modifications are often extremely

important in controlling the activity states and spatial distributions of signaling proteins in cells. The phenotype of a cell correlates more tightly with the amount of active signaling proteins than it does with their total expression levels. We have commonly observed inverse relationships between changes in the active phosphorylated forms of targets proteins and their overall levels. In hindsight, this is not surprising, since cells probably maintain a reserve of inactive protein that is poised for rapid stimulation within seconds after they are needed. Once activated by phosphorylation, they may also become tagged for proteolysis.

Fourthly, genetic changes may be detectable in tumor tissue biopsies, but blood and other bodily fluids contain little or no mRNA for diagnostic purposes. By contrast, protein is readily found in serum, cerebral spinal fluid, saliva, urine, tears, milk, nipple aspirates, semen, vaginal secretions and sweat.

Conventional Proteomics – 2D Gel Electrophoresis

Sodium dodecyl sulphate - polyacrylamide gel electrophoresis (SDS-PAGE) has become the standard method in the field for separation of proteins on the basis of their size for analytical and preparative purposes (9). This widely used technique relies on the sieving effect of a polyacrylamide gel when proteins coated with the negatively-charged detergent SDS are drawn through the gel in an electric field. Smaller sized proteins are able to migrate through the gel faster than larger sized proteins. Proteins that differ by as little as a few hundred Daltons can be resolved by this method. (Most proteins exhibit molecular masses in the forty to fifty thousand Dalton range.) Protein staining methods permit the visualization of discreet proteins in the gel as individual bands in a bar-code like pattern. When these proteins are transferred from the SDS-PAGE gel onto a nitrocellulose membrane, the locations of specific proteins can be identified with antibodies by an immunoblotting procedure commonly referred to as Western blotting (10).

Most proteomics analyses are based on 2D PAGE using the method Dr. Patrick O'Farrell (11) described more than 30 years ago. This 2D gel technique initially involves the separation of proteins based on their intrinsic charge in a pH gradient within a tube gel. Proteins migrate through the isoelectric focusing gel in the presence of an electric field until they encounter a pH at which they no longer possess a net charge. This pH is the isoelectric point of a protein, and it is a distinguishing characteristic. Following electrophoresis in the first dimension, the isoelectric focusing tube gel is applied length-wise to the top of an SDS-PAGE gel, and electrophoresis is continued into the second dimension. When the 2D gel is stained with sensitive-dyes (e.g. based on silver reagent), the various proteins inside a cell can be visualized as resolved spots. The greater amount of a given protein within a cell-derived sample, the larger and darker its specific spot appears. Silver-staining of a 2D gel can be used to track the expression of proteins and their covalent modification such as by phosphorylation. When a protein is phosphorylated, its intrinsic charge is altered and this results in a shift in the migration position of the protein in the 2D gel. If the protein samples have been obtained from cells that have been incubated with radioactive [^{32}P]orthophosphate, then the 2D gel can be exposed to x-ray film, and the ^{32}P -labeled phosphoproteins can be specifically detected. The more that a protein is phosphorylated or prevalent, the larger and more intense the spot on the x-ray film. Alternative methods for detection of phosphoproteins include the

use of Pro-Q Diamond stain from Invitrogen (Hopkinton, MA) or phospho-site specific antibodies.

For protein spots that can be detected and unambiguously identified, the O'Farrell 2D gel approach is a powerful way of monitoring the expression and regulation of potentially hundreds of proteins simultaneously. Public web-based databases have been created that document the identification of over a thousand different proteins on 2D PAGE proteomic maps (12). However, the positions of scarcely more than a few dozen protein kinases have been deduced. This reflects the fact that like most signal transduction proteins, protein kinases are present at very minute levels in cells, and are often undetectable by even such sensitive protein dyes as silver-stain. Typically, signaling proteins are commonly produced at a hundred- to a thousand-fold lower levels than structural proteins and metabolic pathway enzymes. Consequently, these signal transduction proteins are usually overlooked using the traditional proteomics approaches. Therefore, it is often necessary to incorporate selective enrichment techniques as a preliminary step prior to 2D PAGE.

In recent years, mass spectrometry (MS) such as MALDI-TOF has emerged as a very sensitive and powerful method to identify proteins that are resolved by 1D or 2D gel electrophoresis (13). It is now routine to use proteolytic enzymes such as trypsin to cleave eluted proteins from gels into smaller peptides that can be resolved by MS and accurately measured to four decimal places for their charge to mass ratios. Since the charge to mass ratio of all of the tryptic fragments of the proteins predicted to be encoded by the human genome can be calculated and is available in databases such as MASCOT (Matrix Science, London, UK), it is usually possible to immediately assign the identities of several proteins contained within a sample by mass fingerprinting.

While the combination of 2D PAGE and MS can be used to identify thousands of proteins within a cell or tissue lysate, this method is still laborious, expensive, non-quantitative and highly impractical for comparisons of large numbers of biological samples. In fact, it is probably extremely misleading. The low abundance of signaling proteins poses a very serious issue for analyses by 2D PAGE (14). The human genome encodes an estimated 30,000 proteins, and alternative splicing generates five isoforms on average for each gene. Furthermore, the typical phosphoprotein is likely to be phosphorylated at 10 or more separate sites. Moreover, there are many other forms of covalent modification of proteins that can alter their mobilities on 2D PAGE gels. Consequently, the estimated number of distinct protein species within any given cell or tissue type is likely to exceed 100,000.

At best, 2D PAGE can resolve about 8,000 protein spots. Therefore, on average, each spot may contain more than 10 different proteins, and following trypsin treatment, could generate over 100 different peptides for resolution and detection within a single mass spectrometry analysis. The signals from tryptic peptides generated from structural proteins and metabolic pathway enzymes are very likely to swamp any signals arising from low abundance signaling proteins. Another problem is that many proteins precipitate during the initial isoelectric focusing step. Other proteins possess very high or low isoelectric points such that they do not enter the second dimension of the 2D PAGE gel and are missed. Very high molecular mass proteins are also poorly resolved.

Quantitation of protein expression by 2D PAGE and silver-staining can only be accurately performed if all of the spots that arise from a given target protein are tracked, and there is high confidence that essentially all of the signal is attributable to that protein in each spot. Except for only the most highly abundant proteins, this is pretty much impossible.

It is tempting to speculate that the leftward mobility of proteins in some silver-stained spots on 2D PAGE arises from their progressive phosphorylation. However, it should be borne in mind that each spot contains a mixed population of phospho-forms that are differentially phosphorylated at multiple sites, even though they share a common net charge. Consequently, one cannot make any statement about the phosphorylation of proteins at specific sites following 2D PAGE where the proteins are non-specifically visualized by silver stain, or directly for phosphorylation by autoradiography of resolved lysate proteins from [³²P]orthophosphate-labeled cells or by detection with Pro-Q Diamond stain. These shortcomings seriously compromise the utility of 2D PAGE for quantitative analyses despite its widespread use for proteomics studies.

When specific enrichment and labeling methods are used to purify protein samples prior to MS, it is feasible to perform semi-quantitative measurements using MS. For example, 462 proteins were analyzed in stably transfected cell lines overexpressing the ErbB2 (Neu, HER2) receptor-tyrosine kinase or an empty vector by using the SILAC (stable isotope labeling with amino acids in cell culture) method (15). Of these, 198 showed a significant increase in tyrosine phosphorylation in ErbB2-overexpressing cells, and 81 showed a significant decrease in phosphorylation.

Antibodies – The Gold Standard for Proteomics Probes

Often, it is only feasible to identify the locations of low abundance cell signaling proteins on 1D and 2D gels by immunoblotting analysis. Western blotting analysis following electrophoresis is completely reliant on the availability of specific and potent antibodies. These are usually produced in rabbits, mice or goats with short synthetic peptides of 10-20 amino acids long that correspond to a portion of the target protein. Alternatively, monoclonal antibodies are made by mouse and rabbit hybridoma B cells against whole target proteins. It typically takes 4 to 6 months to produce high affinity antibodies, and more often than not, the antibodies that are generated are non-specific and/or impotent. Kinexus has independently tested more than 3000 commercial antibodies with a rejection rate of greater than 75%. Nevertheless, antibodies are the best probes available for specific detection and quantification of proteins.

The detection of phosphopeptides from phosphoproteins by MS is especially problematic due to their relatively low abundance when compared with non-phosphorylated peptides within samples (16). Because the presence of other peptides can suppress the ability to detect phosphopeptides by MS, procedures must be employed to specifically enrich phosphoproteins and phosphopeptides prior to MS. In this regard, phosphite-specific antibodies and immobilized metal-affinity columns have been particularly useful (17). Over 1000 phospho-site antibodies are commercially available for several hundred signaling proteins. However, these reagents are costly to purchase, in part due to the need to affinity purify these antibodies over two columns, i.e. one with the dephospho-form of the immunogenic peptide and the other column with the phosphorylated form of this peptide. This results in very low yields for phosphite-

specific antibodies. Less discriminating monoclonal pan-phosphotyrosine-specific antibodies such as 4G10 and PY20 have proven to be very useful for tracking protein-tyrosine phosphorylation in general, in part due to the extremely low levels of this form of phosphorylation. In most cell types, protein-tyrosine phosphorylation has been estimated to be 2000-fold lower than protein-serine or protein-threonine phosphorylation (18), although in activated platelets the levels of protein-tyrosine phosphorylation are markedly higher (19). There are also pan phospho-serine and phospho-threonine-specific antibodies that have been successfully used to concentrate phosphoproteins prior to their identification by MS (20).

An innovative approach to quantifying the expression and phosphorylation states of proteins is through the use of “Liquid Chip” technology from Luminex (Austin, TX). This instrument can in principle analyze up to 100 different target proteins simultaneously in a complex mixture using beads that can be coated with specific capture probes (typically antibodies). The presence of the captured protein is detected by its subsequent binding of a reporter probe (typically a biotinylated antibody, which could be bound to fluorescently labeled avidin). The amount of signal from the reporter antibody bound to each bead is quantified as it passes through a narrow orifice in a bead sorter with a two laser beam detector (one beam identifies the bead, the other beam records the amount of reporter antibody bound). Several different companies (e.g. Invitrogen (Hopkinton, MA), Millipore (Billerica, MA), Becton Dickinson (Franklin Lakes, NJ)) offering specific assays for kinases and other signaling proteins that can be used with the Luminex instrument and related detectors. However, there are only a limited number of suitable antibody pairs (capture antibody and reporter antibody) that are commercially available. Another technical barrier appears to be a practical limit to the numbers of antibodies (a maximum of about 2 dozen) that can be mixed together without extensive cross-reactivity that renders high backgrounds and high rates of false positive signals. The Luminex system is also not easily adapted for high throughput robotics-assisted analyses. Due to these limitations, we feel that this technology platform will have a more restricted utility relative to protein microarrays.

Antibody Microarrays

Antibody microarrays are enticing due to the higher numbers of proteins that could be tracked simultaneously, their economy of scale, and their high throughput potential with automation (21,21). It can be estimated that 100 µg of an antibody may be sufficient for spotting tens of thousands of glass slides. In principle, antibody microarrays should be an order of magnitude more powerful than gene microarrays. Apart from being able to quantify the actual levels of proteins, antibody microarrays could also be used to track post-translational modifications such as phosphorylation (with phospho-site-specific antibodies), subcellular location (by pre-fractionation of cellular extracts), protein-protein interactions and drug-protein interactions (by affinity chromatography prior to microarray analyses). Sample preparation for protein microarray analysis should also be faster and less expensive than gene microarrays, and require less biopsy material.

Presently, only Clontech (Mountain View, CA) and Sigma-Aldrich (St. Louis, MO) sell antibody microarrays that can track cell signaling proteins. For both of these commercial antibody microarrays, the lysates from control and experimentally treated cells are pre-labeled with different dyes (e.g. Cy3 and Cy5), and then mixed together for

incubation with the same antibody spots. If there are differences in the amounts of target proteins between the samples, then the competition for the various antibodies allows for the dye signal from one sample to predominate over the dye signal from the other sample. Because diverse dyes have different efficiencies in labeling proteins, it is a recommended practice to validate the initial experimental results with these antibody microarrays with a second experiment in which the dyes are reversed between the control and experimental samples. Presently, there are relatively few publications that describe the use of the Clontech (23,24) and Sigma-Aldrich Panorama antibody microarrays (25,26). It is also feasible to avoid dye labeling of proteins prior to their incubation with antibody microarrays, and use surface plasmon resonance (SPR) for the detection of captured proteins instead (27).

The biggest challenge for antibody microarrays is to improve the accuracy of the results that are generated by this approach with better antibodies. In contrast to DNA or other oligonucleotide probes deployed in gene microarrays, antibody probes are often non-specific, as well as expensive (i.e. thousands of dollars) and time consuming (several months) to produce. Validation of key antibody microarray results by an alternative strategy such as Western blotting is essential, since some signals from the microarrays may arise by antibody cross-reactivity. Another complication is that antibody microarrays rely on the use of non-denatured protein samples, and epitopes on proteins may be masked in their native forms. This is especially problematic if the target proteins are complexed with other proteins, which is likely to be very common. For example, at least 137 of the known protein kinases have been reported to occur in dimeric or multimeric forms, and based on their homology with related kinases, most protein kinases probably reside in complexes (28). As shown in Figure 1, these associated proteins may contribute to the signals detected on a microarray, since they are also dye-labeled.

Kinexus Antibody-based Integrated Discovery Platform

While some laboratories have the necessary specialized equipment and software to scan and analyze microarrays, most are not set up to conduct these types of experiments. Furthermore, as outlined above, there are many pitfalls and associated costs with performing antibody microarray analyses and follow up validation studies. In view of this, Kinexus Bioinformatics Corporation launched its Kinex™ antibody microarray services in combination with its Kinetworks™ multi-immunoblotting services as a cost effective solution for academic and industrial laboratories to conduct systems proteomics research. Kinexus has provided its Kinetworks™ services to over 800 laboratories worldwide, and it has generated over 10,000 multi-immunoblots over the last 7 years. Much of the resulting data with quantification of the expression and phosphorylation levels of hundreds of signaling proteins is available to the scientific community on-line through our unique KiNET databank (www.kinexus.ca/kinet). In the balance of this chapter, we will provide an example of a case study in which our proteomics discovery platform was applied to identify biomarkers for the action of a commonly investigated growth factor in a well studied human tumor cell line.

Kinex™ Antibody Microarray Analysis of EGF-treated A431 Cells

Epidermal growth factor (EGF) is one of the best characterized of the growth factors that binds to receptor-tyrosine kinases, and there has been extensive studies of the

signaling pathways that it evokes. Upon ligand binding, the EGF receptor dimerizes, autophosphorylates itself, and recruits a cascade of signaling proteins to transmit potent mitogenic signals in many cellular systems (29-32). A431 cells were originally isolated from the vulva epidermoid carcinoma of an 85 year old female. The EGF receptor is amplified, rearranged and truncated in A431 cells, resulting in over 30-fold higher levels of mRNA for this receptor (33-35). Like other cells that highly overexpress the EGF receptor (36), EGF treatment of A431 cells results in induction of apoptosis (37,38). Recently, a new and sensitive liquid chromatography-MS platform, Extended Range Proteomic Analysis (ERPA), was used to identify 13 phosphorylation sites and 10 extracellular domain N-glycan sites in the EGF receptor in A431 cells treated with EGF (39,40). In the same study (40), 19 proteins were identified that associated with the EGF stimulated EGF receptor. The SILAC method combined with MS has also been successfully used to identify 81 signaling proteins that became tyrosine phosphorylated in response to EGF activation of cultured cells (41). We exploited the A431 cell system to explore the regulation of cell signaling in response to short term treatment with 20 nM EGF for 10 min using the Kinex™ antibody microarray. Protein microarrays have also been employed to study EGF signaling previously (42).

The Kinex™ antibody microarrays are printed in quadruplicate in 32 grids of 8 X 12 spots each on plastic microscope slide-sized chips with 603 antibodies from over 20 different commercial suppliers. These polyclonal and monoclonal antibodies were carefully selected, because they have been highly validated in-house at Kinexus to perform well on Western blots. They included 346 pan-specific antibodies for measurement of the expressions of 240 protein kinases and 106 other signaling proteins, as well as 257 phospho-site-specific antibodies.

To perform a Kinex™ analysis, the lysates with 50 µg protein each from both the untreated (control) and EGF-treated A431 cells were labeled with the same proprietary fluorescent dye. Each sample was separately applied to opposite sides of the antibody microarray that contains a dam to prevent mixing of the samples. Following incubation of the A431 cell samples with the Kinex™ chip, the unbound proteins were washed away, and the chips were scanned with a Perkin-Elmer ScanArray Express Reader. Image analysis of the TIF files that were produced were performed with ImGene 7.0 software from BioDiscovery (El Segundo, CA). For the purposes of presentation in Figure 2, the separate scan images of four of the grids with the control and EGF treated samples were overlaid and slightly staggered so that they could be compared. The EGF-treated sample spots are shown in grey, where as the untreated sample spots appear in black. Duplicate antibodies are printed as adjacent spots. Quantification of the signal intensity of all of the detected spots revealed that the difference between duplicates was within 10% for half of all of the antibodies used. Over 93% of the antibodies detected the binding of dye-labeled proteins from the A431 cell lysates with 100 or more counts. The highest signal observed was 2636 counts, and the lowest reproducible signal was around 30 counts, so there was a 100-fold range of linear detection of protein binding to the Kinex™ antibody microarray.

Table 1 provides a selective listing of all of the antibodies that revealed EGF induced changes in target protein expression or phosphorylation that were 33% or greater. For the generation of these finding, the percentage change from control (%CFC) was the averaged result from the analyses of two separate experiments performed on different occasions with two chips. Common to both experiments, 6.5% of the antibodies revealed

greater than 25 %CFC increases and 5.8% of the antibodies revealed more than 25 %CFC decreases in signal detection. Most of the EGF-induced increases in %CFC were in protein phosphorylation detection (8.2% of 257 phospho-site antibodies), whereas the EGF reductions in %CFC were mainly in protein expression (8.7% of 346 pan-antibodies). Roughly 67% of the phospho-site and pan-specific antibodies showed less than 25 %CFC in both experiments.

It is remarkable that EGF seemed to induced so many apparent changes in protein expression within 10 minutes of initial exposure to the A431 cells. The most likely correct interpretation of these findings is that the growth factor treatment did not alter the synthesis or degradation of these signaling proteins. Rather the treatment probably induced radical changes in complex formation amongst these signaling proteins. Since their associated proteins also contribute to the total signals recorded for many of the antibody spots, their binding to or dissociation from the target proteins would produce apparent changes in protein expression. While this may undermine the use of antibody microarrays to accurately track protein expression, it demonstrates the power of this technology to sensitively reveal changes in protein-protein interactions. Such changes could still prove to be useful markers of drug action or disease. To more precisely track target proteins for expression changes, it would be desirable to use denatured proteins that are dissociated from other proteins. However, it is tricky to find conditions to unfold proteins without inducing their precipitation, and the inclusion of detergents, for example, might interfere with the binding of target proteins to the antibodies on the microarray. Follow up Western blotting is necessary to evaluate the true nature of the EGF induced changes observed with the pan-specific antibodies.

Kinetworks™ Multi-immunoblotting Analysis of EGF-treated A431 Cells

Kinexus has developed a multi-immunoblotting process trademarked Kinetworks™, which permits the quantitative analyses of up to 50 or more target proteins at once on the same SDS-PAGE gel (43). With this method, a sample is loaded within a single lane that spans the width of the gel, and following SDS-PAGE, the resolved proteins are electroeluted onto a nitrocellulose membrane. Subsequently, an Immunitics (Cambridge, MA) plexiglas manifold with typically 20 separate channels is overlaid over the membrane, and different mixtures of antibodies are applied to each slot of the immunoblotter. It is critical that none of the non-specific cross-reactive proteins detected with antibodies in each mixture co-migrate with target proteins in the same lane, otherwise this generates false positives. Therefore, exhaustive testing of the antibody mixtures with diverse cells and tissues is required. Following incubation of the immunoblot with secondary antibodies and detection by enhanced chemiluminescence (ECL), the resulting blot looks like a 2D gel, but with discreet bands rather than fuzzy spots.

The multi-immunoblotting approach is cheaper, faster, more sensitive for the detection of protein kinases and other low abundance signal transduction proteins, more versatile and offers greater reproducibility than conventional 2D gel methods. This technique can be applied to cell or tissue samples, including patient biopsy material. With the Kinetworks™ mini-SDS-PAGE gel format, only 300 µg of crude cell lysate is required to probe the expression, state of phosphorylation or cleavage of target proteins. The signals of immunoreactive proteins detected by ECL and a fluorescence scanner can

be quantified over a 2000-fold range with linearity. The results for the same sample analyzed by Kinetworks™ on different days typically vary by 5-20% depending on the signal intensity of each immunoreactive protein. Kinexus has performed over 10,000 Kinetworks™ analyses to examine the expression and phosphorylation of protein kinases, protein phosphatases, cell cycle, stress and apoptosis proteins.

Figure 3 shows the results of 5 different Kinetworks™ KPSS Phospho-Site screens applied to the analyses of phosphoproteins in lysates from untreated A431 cells, and cells exposed to 20 nM EGF for 10 minutes. Each of these Kinetworks™ KPSS screens were capable of scanning 35 to 40 known phospho-sites. There was some redundancy in the coverage of phospho-sites by these screens, which together used over 133 distinct phospho-site antibodies. Approximately 19% of these antibodies did not detect their phosphoprotein targets in the A431 cells. Only the results for the detected target phosphoproteins are quantified in Table 2. EGF treatment resulted in greater than 25 %CFC increases in phosphorylation levels for 30% of the target phospho-sites, and more than 25 %CFC reductions in phosphorylation for 17% of the target phospho-sites. Extensive Google searches revealed that of the 40 detected phospho-sites in Table 2 that showed greater than 25 %CFC increases, EGF has been found to stimulate the phosphorylation of 23 of them in previous studies in other tumor cell lines (e.g. Erk1, Erk2, RSK, PDK1, PKB/Akt). EGF also induces increases in the phosphorylation of the following phospho-sites that do not appear to have been reported previously: Grk2 S670; Hsp25 S86; Hsp27 S15; Hsp27 S78; IRS1 Y612; IRS1 Y1179; MEK1 T385; MLK3 T277+S281; MRLC2 S18; p53 S392; NR1 S896; PED15 S116; PKA C β S338; PKC γ T514; PKC γ T655; PKC η S674; and Rad17 S645. Of the 34 phospho-sites that EGF treatment of A431 cells caused greater than 25% reductions in their phosphorylation signals, 11 have actually been reported to be increased by EGF in other tumor cell lines. These conflicting phospho-sites corresponded to: 4E-BP1 S65; cofilin 1 S3; CREB S133; FAK Y576; FAK S910; GSK3 α S21; JNK T183+Y185; PKC ϵ S729; Rac1/Cdc42 S71; S6K2 p85 T252; and STAT1 S727. The other observed EGF induced decreases in protein phosphorylation shown in Table 2 do not appear to have been previously reported.

We can ascribe a high level of confidence that the target phospho-sites were accurately tracked in the experiments shown in Figure 3, in part because the molecular masses of the detected phosphoproteins were monitored in parallel by the immunoblotting. However, it should be appreciated that Western blot analysis with phospho-site antibodies alone cannot differentiate whether the altered immunoreactivity signals reflected a change in the stoichiometry of phosphorylation of target proteins or an alteration in the total amount of the target proteins (i.e. the stoichiometry may be unaffected). It is necessary to evaluate whether there are changes in the overall expression levels of the target proteins to ascertain the true extent of their phosphorylation.

Comparison of Antibody Microarray and Immunoblotting Results for EGF-treated A431 Cells

The previous Kinetwork™ multi-immunoblotting studies afforded the opportunity to critically evaluate the findings derived from the Kinex™ antibody microarray experiments with the EGF-treated A431 cell lysates. The rightmost column in Table 1

shows the %CFC induced by EGF treatment of the A431 cells in phospho-sites that were examined by immunoblotting. Of the 34 top phospho-site changes identified by the antibody microarray, 15 had positive correlations (i.e. similar trends in %CFC) and 14 had negative correlations (i.e. dissimilar trends such as an increase in %CFC from the microarray but no change or a decrease based on immunoblotting). Five of the target phospho-sites showed no immunoreactivity signals on the immunoblots. Similar findings were observed when the overall results for the antibody microarray data were examined by validation studies by immunoblotting with 154 different phospho-site antibodies: 41% of the antibody microarray results were confirmed by immunoblotting; 42% of the antibody microarray results did not match the trends shown by immunoblotting; and 17% of the phospho-sites detected on the microarray could not be visualized by immunoblotting.

In view of the higher concentrations of antibodies used in the microarray platform as compared to immunoblotting, it is not surprising that the antibody microarray was much more sensitive for protein detection. The high degree of false positives with the antibody microarray is also not unexpected in view of the considerations illustrated in Figure 1. In particular, antibodies can demonstrate high cross-reactivity with other proteins. Furthermore, it is the amount of dye that is bound to proteins captured by the immobilized antibodies on the microarray that is specifically tracked. Since non-denatured proteins were examined with the antibody microarray, many of the target proteins should be expected to occur in complexes with other proteins. EGF induced changes in protein-protein interactions in these complexes will confound interpretation of the findings from the antibody microarray.

The occurrence of the protein complexes also increased the probability of false negatives, since the epitopes recognized by the microarray antibodies may be masked by associated proteins. Furthermore, it is possible that some of the antibody epitopes may not be accessible in the native folded structure of monomeric target proteins depending on their state of activation. To get a sense of the false negative rate, we examined the key changes in protein phosphorylation that were evident by immunoblotting and compared these to the corresponding results evident from the antibody microarray data. Of 89 phospho-site signal changes induced by EGF that were detected by the Kinetworks™ multi-immunoblots in A431 cell lysates by immunoblotting, only 15% of these EGF responses (i.e. greater than 25 %CFC increase or decrease) were closely matched by the Kinex™ antibody microarray findings. By contrast, 80% of the phospho-sites that failed to show EGF induced differences by multi-immunoblotting (i.e. less than 25 %CFC increase or decrease), also demonstrate little (less than 25 %CFC) if any changes by the antibody microarray analysis. The multi-immunoblotting approach was much more accurate in picking up changes in protein phosphorylation than the antibody microarray.

This inherent problem, which is associated with working with native, non-denatured proteins in antibody microarrays, is strongly demonstrated in the case of Erk1 and Erk2 phosphorylation. On the one hand, the Kinetworks™ multi-immunoblotting data shown in Table 2 clearly reveals EGF induced nearly 3-fold increases in the phosphorylations of both MAP kinases at their stimulatory phospho-sites in A431 cells. On the other hand, there were no indications of EGF increased phosphorylations of Erk1 and Erk2 from the Kinex™ antibody microarray, despite the fact that this microarray features anti-Erk1/2 T202+Y204/T185+Y187 phospho-site antibodies from four different commercial

suppliers as separate spots. We did observe EGF triggered apparent decreases of 34% to 50% in the total levels of Erk1 and Erk2, respectively, with the antibody microarray. The explanation for these findings may arise from the fact that these MAP kinases occur in heterodimeric complexes with MEK1 and MEK2 in their inactive states, and upon their phosphorylation, they form homodimeric active complexes (28). In their active, complexed forms, their phosphorylation sites may not be accessible to antibodies. Moreover, epitopes for the pan-specific MAP kinase antibodies may also be masked in the Erk1-Erk1 or Erk2-Erk2 dimers. The ability to dissociate such complexes would markedly improve the reliability of antibody microarrays to quantify the expression and phosphorylation states of target proteins.

Antibody-driven Protein and Phospho-site Discovery

One of the serendipitous benefits of the Kinetworks™ multi-blot analysis is the detection of unknown cross-reactive proteins. Those unidentified immunoreactive proteins that change in expression or phosphorylation in response to a disease condition or treatment with a drug can be purified or at least tracked with the cross-reactive antibodies that detected them in the first place. This permits the identification of these proteins by MS or by direct protein sequencing by standard Edman degradation methodology. In the case of phospho-site antibodies, the epitope of the detection antibody is usually known, so it is often possible to predict the location of the phosphorylation site within the identified protein. The same antibody could be useful for subsequent immunohistochemistry studies to precisely identify the cell type and subcellular compartment within which the phosphorylation has occurred.

For example, we successfully used this approach to discover Ser-4 as a novel site for phosphorylation of B23 (also known as nucleophosmin) by its cross-reactivity with an antibody originally developed to recognize the MEK1 S217+S221 phospho-sites (44). From the amino acid sequences surrounding the B23 S4 site, we deduced polo-like kinase as a possible candidate for catalyzing its phosphorylation, which we confirmed by multiple strategies, including RNAsi. By mutational analyses, we established that S4 phosphorylation of B23 is critical for centrosome duplication prior to mitosis.

In the rightmost panels in Figure 3, question marks have been placed next to more than 30 antibody cross-reactive proteins that demonstrated EGF-induced increases or decreases in phosphorylation in the A431 cells. Enrichment of these phosphoproteins by immunoaffinity and their identification by MS could yield new missing links in EGF signaling pathways.

Variation of EGF Signaling Pathways in Diverse Cell Types

As mentioned above, 11 of the phospho-sites that displayed reduced immunoreactivity signals by Kinetworks™ multi-immunoblotting in EGF-treated A431 cells were previously shown to undergo EGF induced increases in phosphorylation in other tumor cell types. This may reflect the cell-specific nature of signaling pathways. The same growth factor or drug treatment can elicit extremely different responses in diverse cells that differentially express signal transduction proteins. To explore this phenomena, we took advantage of the KiNET on-line databank to examine how EGF affected protein phosphorylation in other tumor cell lines using the same antibodies and conditions used to investigate EGF action in A431 cells. From this query of KiNET, we

found data for EGF's effects on 32 phospho-sites in seven other tumor cell lines and this is summarized in Table 3. It is evident that there is a large diversity in the behavior of these phospho-sites to similar concentrations of EGF and time of exposure across the tumor cell lines. The most reliable biomarkers of EGF stimulation were the increased phosphorylations of Erk1 T185+Y187, Erk2 T202+Y204, MEK1 S217+S221, PKB α S473, STAT3 S727, Raf1 S259, Rb S807+S811, p38 α MAPK T180+Y182, adducin α S726 and Rb S780, and decreased phosphorylation of CREB S133. However, for each of these phospho-sites, there are examples of tumor cells where EGF had no or an opposite effect. This demonstrates the importance of working with a diversified panel of biomarkers to track the actions of any particular hormone or drug.

The need to identify a panel of biomarkers to reliably diagnose a particular disease in patient biopsy material is revealed in another yet unpublished study that Kinexus has conducted to examine phosphoprotein patterns in human tumor cells by Kinetworks™ multiblotting analyses. Over 80 different phospho-sites were profiled across 40 well characterized human tumor breast cancer cell lines. Not one of the cell lines showed a similar pattern of phospho-site signals with another. This supports the possibility that every human cancer is distinct at the molecular level, and underscores the need for personalized medicine approaches.

Conclusions

Antibody microarrays have the potential to transform proteomics studies and facilitate system biology research. The identification of reliable antibody probes and sample preparation remain significant obstacles in realization of the full potential of these protein microarrays. In the present study, it was estimated that for the assessment of EGF actions in the A431 tumor cell line, about 44% of the changes in protein phosphorylation evident from the Kinex™ antibody microarray could be validated by immunoblotting. However, 85% of the phosphorylation differences that were identified by Kinetworks™ multi-immunoblotting were missed by the antibody microarray. Nevertheless, in view of the high sensitivity, low cost and wide scope of the analyses provided by the antibody microarray approach, this represents a very effective strategy for biomarker discovery, especially when this is accompanied by rapid validation by immunoblotting. Once a cell or tissue type become well characterized for the reliability of the antibody probes for that system, the antibody microarray should be a powerful tool for mapping cell signaling pathways and monitoring their disruptions in complex diseases such as cancer.

Acknowledgements

This work was supported by a grant from the Canadian Institutes for Health Research to SP and a grant from the National Research Council of Canada Industrial Research Assistance Program to Kinexus.

References

1. Manning G, Whyte DB, Martinez R, Hunter T, Sudarsanam S. The protein kinase complement of the human genome. *Science*. 2002; 298:1912-1934.
2. Kostich M, English J, Madison V, Gheyas F, Wang L, Qiu P, Greene J, Laz, TM. Human members of the eukaryotic protein kinase family. *Genome Biol.* 2002; 3:

RESEARCH0043.

3. Wolstencroft KJ, Stevens R, Taberero A, Brass, A. PhosphaBase: An ontology-driven database resource for protein phosphatases. *Proteins Structure Function Bioinformatics*. 2004; 58:290-294.
4. Pelech SL. Kinase profiling; The mysteries unraveled. *Future Pharmaceuticals*. 2006; 1:23-25.
5. Mukherji M. Phosphoproteomics in analyzing signaling pathways. *Expert Rev Proteomics*. 2005; 2:117-128.
6. Via MC. Kinases: From targets to therapeutics. *Cambridge Health Institutes Insight Reports*. 2003; 1-124.
7. Griffin TJ, Gygi SP, Ideker T, Rist B, Eng J, Hood L, Aebersold R. Complementary profiling of gene expression at the transcriptome and proteome levels in *Saccharomyces cerevisiae*. *Mol Cell Proteomics*. 2002; 1:323-333.
8. Yoo GH, Piechocki MP, Ensley JF, Nguyen T, Oliver J, Meng H, Kewson D, Shibuya TY, Lonardo F, Tainsky MA. Docetaxel induced gene expression patterns in head and neck squamous cell carcinoma using cDNA microarray and PowerBlot. *Clin Cancer Res*. 2002; 8:3910-3921.
9. Laemmli UK. Cleavage of structural proteins during the assembly of the head of Bacteriophage T4. *Nature*. 1970; 227:680-685.
10. Burnette WN. "Western blotting": electrophoretic transfer of proteins from sodium dodecyl sulfate gels to unmodified nitrocellulose and radiographic detection with antibody and radioiodinated protein A. *Anal Biochem*. 1981; 112:195-203.
11. O'Farrell PH. High resolution two-dimensional electrophoresis of proteins. *J Biol Chem*. 1975; 250:4007-4021.
12. Celis JE, Østergaard M, Jensen NA, Gromova I, Rasmussen HH, Gromov P. Human and mouse proteomic databases: novel resources in the protein universe. *FEBS Letters*. 1998; 430:64-72.
13. Aebersold R, Mann M. Mass spectrometry-based proteomics. *Nature* 2003; 422:198-207.
14. Gygi SP, Corthals GL, Zhang Y, Rochon Y, Aebersold R. Evaluation of two-dimensional gel electrophoresis-based proteome analysis technology. (2000) *Proc Natl Acad Sci USA*. 2000; 97:9390-9395.
15. Bose R, Molina H, Patterson AS, Bitok JK, Periaswamy B, Bader JS, Pandey A, Cole PA. Phosphoproteomic analysis of Her2/neu signaling and inhibition. *Proc Natl Acad Sci USA*. 2006; 103:9773-9778.
16. Annan RS, Huddleston MJ, Verma R, Deshaies RJ, Carr SA. A multidimensional electrospray MS-based approach to phosphopeptide mapping. *Anal Chem*. 2001; 73:393-404.
17. Ficarro SB, McClelland ML, Stukenberg PT, Burke DJ, Ross MM, Shabanowitz J, Hunt DF, White FM. Phosphoproteome analysis by mass spectrometry and its application to *Saccharomyces cerevisiae*. *Nat Biotechnol*. 2002; 20:301-305.
18. Hunter T. The Croonian Lecture 1997. *Philos Trans R Soc Lond B Biol Sci*. 1998; 353:583-605.
19. Maguire PB, Wynne KJ, Harney DF, O'Donoghue NM, Stephens G, Fitzgerald DJ. Identification of the phosphotyrosine proteome. *Proteomics*. 2002; 2:642-648.

20. Gronborg M, Kristiansen TZ, Stensballe A, Andersen JS, Ohara O, Mann M, Jensen ON, Pandey A. A mass spectrometry-based proteomic approach for identification of serine/threonine-phosphorylated proteins by enrichment with phospho-specific antibodies: identification of a novel protein, Frigg, as a protein kinase A substrate. *Mol Cell Proteomics*. 2002; 1:517-527.
21. Wingren C, Borrebaeck CA. High-throughput proteomics using antibody microarrays. *Expert Rev Proteomics*. 2004; 1:355-364.
22. Borrebaeck CA. Antibody microarray-based oncoproteomics. *Expert Opin Biol Ther*. 2006; 6:833-838.
23. Hudelist G, Pacher-Zavisin M, Singer CF, Holper T, Kubista E, Schreiber M, Manavi M, Bilban M, Czerwenka K. Use of high-throughput protein array for profiling of differentially expressed proteins in normal and malignant breast tissue. *Breast Cancer Res Treat*. 2004; 86:281-291.
24. Ghobrial IM, McCormick DJ, Kaufmann SH, Leontovich AA, Loegering DA, Dai NT, Krajnik KL, Stenson MJ, Melhem MF, Novak AJ, Ansell SM, Witzig TE. Proteomic analysis of mantle-cell lymphoma by protein microarray. *Blood*. 2005; 105:3722-3730.
25. Kopf E, Shnitzer D, Zharhary D. Panorama Ab Microarray Cell Signaling kit: a unique tool for protein expression analysis. *Proteomics*. 2005; 5:2412-2416.
26. Smith L, Watson MB, O'Kane SL, Drew PJ, Lind MJ, Cawkwell L. The analysis of doxorubicin resistance in human breast cancer cells using antibody microarrays. *Mol Cancer Ther*. 2006; 5:2115-2120.
27. Usui-Aoki K, Shimada K, Nagano M, Kawai M, Koga H. A novel approach to protein expression profiling using antibody microarrays combined with surface plasmon resonance technology. *Proteomics*. 2005; 5:2396-2401.
28. Pelech S. Dimerization in protein kinase signaling. *J Biol*. 2006; 5:12.
29. Jorissen RN, Walker F, Pouliot N, Garrett TP, Ward CW, Burgess AW. Epidermal growth factor receptor: mechanisms of activation and signalling. *Exp Cell Res*. 2003; 284:31-53.
30. Holbro T, Hynes NE. ErbB receptors: directing key signaling networks throughout life. *Annu Rev Pharmacol Toxicol*. 2004; 44:195-217.
31. Citri A, Yarden Y. EGF-ERBB signalling: towards the systems level. *Nat Rev Mol Cell Biol*. 2006; 7:505-516.
32. Normanno N, De Luca A, Bianco C, Strizzi L, Mancino M, Maiello MR, Carotenuto A, De Feo G, Caponigro F, Salomon DS. Epidermal growth factor receptor (EGFR) signaling in cancer. *Gene*. 2006; 366:2-16.
33. Lin CR, Chen WS, Krueger W, Stolarsky LS, Weber W, Evans RM, Verma IM, Gill GN, Rosenfeld MG. Expression cloning of human EGF receptor complementary DNA: gene amplification and three related messenger RNA products in A431 cells. *Science*. 1984; 224:843-848.
34. Merlino GT, Xu YH, Ishii S, Clark AJ, Semba K, Toyoshima K, Yamamoto T, Pastan I. Amplification and enhanced expression of the epidermal growth factor receptor gene in A431 human carcinoma cells. *Science*. 1984; 224:417-419.
35. Ullrich A, Coussens L, Hayflick JS, Dull TJ, Gray A, Tam AW, Lee J, Yarden Y, Libermann TA, Schlessinger J, et al. Human epidermal growth factor receptor cDNA sequence and aberrant expression of the amplified gene in A431

- epidermoid carcinoma cells. *Nature*. 1984; 309:418-425.
36. Helseth E, Dalen A, Unsgaard G, Vik E, Helseth A. Overexpression of the epidermal growth factor receptor gene in a human carcinoma cell line, derived from a brain metastasis. *J Neuro-Oncology*. 1989; 7: 81-88.
 37. Gulli LF, Palmer KC, Chen YQ, Reddy KB. Epidermal growth factor-induced apoptosis in A431 cells can be reversed by reducing the tyrosine kinase activity. *Cell Growth Differ*. 1996; 7:173-178.
 38. Smida Rezgui S, Honore S, Rognoni JB, Martin PM, Penel C. Up-regulation of alpha 2 beta 1 integrin cell-surface expression protects A431 cells from epidermal growth factor-induced apoptosis. *Int J Cancer*. 2000; 87:360-367.
 39. Wu SL, Kim J, Hancock WS, Karger B. Extended Range Proteomic Analysis (ERPA): a new and sensitive LC-MS platform for high sequence coverage of complex proteins with extensive post-translational modifications-comprehensive analysis of beta-casein and epidermal growth factor receptor (EGFR). *J Proteome Res*. 2005; 4:1155-1170.
 40. Wu SL, Kim J, Bandle RW, Liotta L, Petricoin E, Karger BL. Dynamic profiling of the post-translational modifications and interaction partners of epidermal growth factor receptor signaling after stimulation by epidermal growth factor using Extended Range Proteomic Analysis (ERPA). *Mol Cell Proteomics*. 2006; 5:1610-1627.
 41. Blagoev B, Ong SE, Kratchmarova I, Mann M. Temporal analysis of phosphotyrosine-dependent signaling networks by quantitative proteomics. *Nat Biotechnol*. 2004; 22:1139-1145.
 42. Espina V, Woodhouse EC, Wulfkuhle J, Asmussen HD, Petricoin EF 3rd, Liotta LA. Protein microarray detection strategies: focus on direct detection technologies. *J Immunol Methods*. 2004; 290:121-133.
 43. Pelech S, Sutter C, Zhang, H. Kinetworks™ protein kinase multiblot analysis. *Methods in Molecular Biology: Cancer Cell Signaling: Methods and Protocols* (Terrian, D.M, ed.) Humana Press, 2003; 218:99-111.
 44. Zhang H, Shi X, Hampong M, Paddon H, Dai W, Pelech SL. Polo-like kinase regulation of centrosomes is mediated through Serine 4 phosphorylation of B23/nucleophosmin. *J Biol Chem*. 2004; 279:35726-35734.

Table Legends

Table 1. Kinex™ antibody microarray detection of key changes in signal transduction protein expression and phosphorylation induced by exposure of A431 cells to 20 nM EGF for 10 min. Values are the averages and ranges of signals recorded from two separate experiments. %CFC refers to the percent change from control (untreated with EGF). Only %CFC that were 33% or greater are shown for 101 target proteins and phospho-sites. For comparison, the %CFC in parallel studies performed by Kinetworks™ multi-immunoblotting are provided for some of the phospho-site antibodies in the rightmost column.

Table 2. Kinetworks™ multi-immunoblotting analysis of changes in signal transduction protein phosphorylation induced by exposure of A431 cells to 20 nM EGF for 10 min.

Values are the averages of recorded ECL signals in counts per minute (cpm), with the number of determinations shown in the rightmost column. %CFC refers to the percent change from control (untreated with EGF). One hundred and eight separate phospho-site antibodies successfully detected their target proteins in these tumor cells.

Table 3. Summary of KiNET query results for EGF induced changes in 32 phospho-sites in 8 different human tumor cell lines. The data was retrieved by query of KiNET at www.kinexus.ca/kinet. The %CFC are shown and increases $\geq 30\%$ are in black boxes, whereas decrease $\geq 30\%$ are in grey boxes. ND = not determined. 0* = no detectable signals. INCREASE = situation where there was no detectable phospho-site signals in the untreated control cells.

Fig. 1. Different scenarios for protein binding to antibody microarrays. The antibodies are developed to recognize the proteins that are similarly labeled with an alphabet character.

Fig. 2. Examples of changes in protein expression and phosphorylation as visualized on 4 of the 16 grids on a Kinex™ antibody microarray. Spots generated from lysates from A431 cells treated with 20 nM EGF for 10 min are shown in grey, whereas the corresponding spots from untreated controls are shown immediately in the row below in black. Each antibody was printed in adjacent duplicate spots. Antibody spots that revealed changes with EGF are boxed and labeled with the identity of the protein antigen. The %CFC values are indicated for selected antibody spots.

Fig. 3. Examples of changes in protein phosphorylation induced by 20 nM EGF for 10 min in A431 cells as visualized by Kineworks™ multi-immunoblotting with KPSS Phospho-Site Screens 7.0, 8.0, 10.0, 11.0 and 12.0. The detected phosphoproteins in untreated cells are indicated in the leftmost panels. EGF induced increases in phosphorylation are boxed, whereas EGF induced decreases in phosphorylation are circled in the rightmost panels. Question marks are located to the left of unknown cross-reactive proteins that are EGF responsive.

Target Protein Name	Phospho Site (Human)	Full Target Protein Name	Swiss-prot Link	Control Signal Average	Control Signal Range	+EGF Average %CFC	+EGF Average %CFC Range	+EGF Immuno-blotting %CFC
Ret	S696	Ret receptor-tyrosine kinase	P07949	400	300	245	244	
Rad17	S645	Rad17 homolog	O75943	447	229	105	98	131
Rb	S612	Retinoblastoma-associated protein 1	P06400	812	478	97	99	-3
ErbB2 [HER2]	Y1248	ErbB2 (Neu, HER2) receptor-tyrosine kinase	P04626	474	33	87	56	-41
RSK1/2	S380/S386	Ribosomal S6 protein-serine kinase 1/2	Q15418	35	3	84	0	82
PKCε	S729	Protein-serine kinase C epsilon	Q02156	173	13	84	25	-100
Rb	S807	Retinoblastoma-associated protein 1	P06400	848	463	82	70	59
PRK1/2 [PKN1/2]	T774	Protein kinase C-related protein-serine kinase 1/2	Q16512	53	1	80	6	-44
Smad1/5/9	S463+S465	SMA- + mothers against decapentaplegic homologs 1/5/9	Q15797	255	3	77	51	
eIF2Bε	S540	Eukaryotic translation initiation factor 2B epsilon	Q13144	273	17	77	1	
Tau	S720	Microtubule-associated protein tau	P10636E	465	25	77	13	
GSK3α/β	Y279/ Y216	Glycogen synthase-serine kinase 3 alpha/beta	P49841	324	134	71	54	10
Vinculin	Y821	Vinculin	P18206E	641	39	68		-8
TyrHyd α	S19	Tyrosine hydroxylase isoform alpha	P07101	217	11	60	18	
FAK	Y577	Focal adhesion protein-tyrosine kinase	Q05397	669	5	59	22	
Histone H2A.X	S139	Histone H2A variant X	P16104	330	157	56	61	
Crystallin αB	S19	Crystallin alpha B (heat-shock 20 kDa like-protein)	P02511	502	87	54	15	
PKCγ	T514	Protein-serine kinase C gamma	Q02156	461	45	48	19	57
PKCζ/λ	T410/T403	Protein-serine kinase C zeta/lambda	Q05513	158	0	44	17	23
Met	Y1230+Y1234+Y1235	Hepatocyte growth factor receptor-tyrosine kinase	P08581	381	5	42	17	
Rb	S780	Retinoblastoma-associated protein 1	P06400	36	7	41	35	39
FAK	Y576	Focal adhesion protein-tyrosine kinase	Q05397	346	3	40	11	
MYPT1	T696	Myosin phosphatase target 1	O14974	294	37	40	5	
B23 (NPM)	T199	B23 (nucleophosmin, numatrin, NO38)	P06748	888	184	40	37	-47
FAK	Y397	Focal adhesion protein-tyrosine kinase	Q05397	312	102	39	38	42
Tau	S530	Microtubule-associated protein tau	P10636E	798	99	39	12	
p38 α/MAPK	T180+Y182	Mitogen-activated protein-serine kinase p38 alpha	Q16539	591	106	38	28	INCR
Met	Y1003	Hepatocyte growth factor receptor-tyrosine kinase	P08581	456	27	37	24	
S6Kα [p70 S6Kα]	T421+S424	p70 ribosomal protein-serine S6 kinase alpha	P23443	399	33	36	30	0
Bad	S99	Bcl2-antagonist of cell death protein	Q92934	733	44	36	13	
FAK	Y425	Focal adhesion protein-tyrosine kinase	Q05397	322	23	36	33	
RSK1/2	S363/S369	Ribosomal S6 protein-serine kinase 1/2	Q15418	560	74	36	5	1
Crystallin αB	S45	Crystallin alpha B (heat-shock 20 kDa like-protein)	P02511	595	1	35	17	
ATM PK	S1981	Ataxia telangiectasia mutated Ser/Thr kinase	Q13315	270	116	-33	38	
Hsp27	S78	Heat shock 27 kDa protein beta 1 (HspB1)	P04792	619	23	-33	0	461
Shc1	Y349+Y350	SH2 domain-containing transforming protein 1	P29353	995	60	-36	6	166
PKCθ	T538	Protein-serine kinase C theta	Q04759	33	5	-38	24	
Synapsin 1	S603	Synapsin 1 isoform la	P17600	12	12	-43	43	
Jun	S63	Jun proto-oncogene-encoded AP1 transcription factor	P05412	104	51	-51	19	
Lyn	Y507	Yes-related protein-tyrosine kinase	P07948	37	21	-53	16	-24
MARCKS	S158+S162	Myristoylated alanine-rich protein kinase C substrate	P29966	31	3	-66	23	2
PACSIN1	Pan-specific	PKC + casein kinase substrate in neurons protein 1	Q9B111	185	128	337	277	
PTP1B	Pan-specific	Protein-tyrosine phosphatase 1B	P18031	651	496	252	247	
PyDK2	Pan-specific	Pyruvate dehydrogenase kinase isoform 2	Q15119	265	155	250	158	
PKA Cα/β	Pan-specific	cAMP-dep. protein kinase catalytic subunit alpha/beta	P17612	518	7	206	209	
CASP7	Pan-specific	Pro-caspase 7 (ICE-LAP3, Mch3)	P55210	22	6	163	24	
Svk	Pan-specific	Spleen protein-tyrosine kinase	P43405	350	224	152	160	
Erk6 [p38γ]	Pan-specific	Mitogen-activated protein kinase p38 gamma (MAPK12)	Q05397	151	22	104	23	
MEK6 [MAP2K6]	Pan-specific	MAP kinase protein-serine kinase 6 (MKK6)	P52564	104	64	91	117	
p16 INK4	Pan-specific	p16 INK4a cyclin-dependent kinase inhibitor (MTS1)	P42771	957	552	86	72	
ROKα [ROCK2]	Pan-specific	RhoA protein-serine kinase alpha (ROCK2)	O75116	732	321	82	60	
MST1	Pan-specific	Mammalian STE20-like protein-serine kinase 1	Q13043	421	16	74	66	
RSK2	Pan-specific	Ribosomal S6 protein-serine kinase 2	P51812	431	233	73	65	
DNAPK	Pan-specific	DNA-activated protein-serine kinase	P78527	287	18	68	27	
p53	Pan-specific	Tumor suppressor protein p53 (antigenNY-CO-13)	P04637	397	31	67	23	
p35	Pan-specific	CDK5 regulatory subunit 1, p35	Q13319	286	141	64	55	
Smac/DIABLO	Pan-specific	Second mitochondria-derived activator of caspase	Q9NR28	281	17	59	15	
FasL	Pan-specific	Tumor necrosis factor ligand, member 6	P48023	885	97	50	12	
MKP2	Pan-specific	MAP kinase phosphatase 2 (VH2)	Q13115	704	218	49	28	
Grp78	Pan-specific	Glucose regulated protein 78	P11021	817	283	48	40	
ERP57	Pan-specific	ER protein 57 kDa (protein disulfide isomerase-assoc. 3)	P30101	126	22	41	46	
NME7	Pan-specific	Nucleotide diphosphate kinase 7 (nm23-H7)	Q9Y5B8	522	175	39	22	
Nek4	Pan-specific	NIMA (never-in-mitosis)-related protein kinase 4	P51957	449	109	39	18	
SIRP	Pan-specific	Substrate of PTP1D phosphatase (SHPS1)	P78324	801	106	38	27	
S6Kβ [p70 S6Kβ]	Pan-specific	p70 ribosomal protein-serine S6 kinase beta	Q9UBS0	363	11	35	6	
ASK1 [MAP3K5]	Pan-specific	Apoptosis signal regulating protein-serine kinase	Q99683	337	18	34	9	
Aik	Pan-specific	Aurora/PL1-related kinase 1	O14965	404	28	34	13	
CASP4	Pan-specific	Pro-caspase 4 (ICH2 protease, ICE(rel)-II)	P49662	705	14	-33	25	
CaMKK[CaMKK2]	Pan-specific	Calmodulin-dependent protein-serine kinase	Q8N5S9	285	0	-33	38	
TBK1	Pan-specific	Tank-binding protein 1	Q9UHD2	423	42	-33	2	
Bax	Pan-specific	Apoptosis regulator Bcl2-associated X protein	Q07812	513	41	-34	31	
Erk1	Pan-specific	Extracellular regulated protein kinase 1 (p44 MAPK)	P27361	252	7	-34	1	
PP2B/Aα	Pan-specific	Protein-serine phosphatase 2B - cat. subunit - alpha	Q08209	66	25	-34	32	
PKCβ	Pan-specific	Protein-serine kinase C beta 1	P05771	472	51	-34	4	
MEK6[MAP2K6]	Pan-specific	MAP kinase protein-serine kinase 6 (MKK6)	P52564	381	42	-35	37	
PAK3	Pan-specific	p21-activated protein-serine kinase 3	O75914	476	19	-35	16	
Aik	Pan-specific	Anaplastic lymphoma kinase	Q9UM73	1405	111	-36	52	
Mcl1	Pan-specific	Myeloid cell leukemia differentiation protein 1	Q07820	380	9	-37	17	
DFF45	Pan-specific	DNA fragmentation factor alpha (ICAD)	O00273	225	31	-38	13	
HO1	Pan-specific	Heme oxygenase 1	P09601	265	13	-38	8	
HO2	Pan-specific	Heme oxygenase 2	P30519	492	44	-38	12	
KHS	Pan-specific	Kinase homologous to SPS1/STE20 (MEKKK5)	Q9Y4K4	351	33	-39	7	
Hsp40	Pan-specific	DnaJ homolog, subfamily B member 1	P25685	397	14	-39	5	
TBK1	Pan-specific	Tank-binding protein 1	Q9UHD2	508	50	-40	33	
14-3-3 ζ	Pan-specific	14-3-3 protein zeta	P63104	428	91	-41	34	
Btk	Pan-specific	Bruton's agammaglobulinemia tyrosine kinase	Q06187	381	61	-41	5	
ROR2	Pan-specific	ROR2 neurotrophic receptor-tyrosine kinase	Q01974	177	88	-41	38	
JAK1	Pan-specific	Janus protein-tyrosine kinase 1	P23458	151	16	-42	19	
ACK1 [ACK]	Pan-specific	Activated p21cdc42Hs protein-serine kinase	Q07912	382	46	-43	32	
Hpk1	Pan-specific	Hematopoietic progenitor protein-serine kinase 1	Q92918	504	3	-43	4	
CaMK1δ	Pan-specific	Calcium/calmodulin-dep. protein-serine kinase 1 delta	Q8IU85	414	99	-43	1	
CASP1	Pan-specific	Pro-caspase 1 (Interleukin-1 beta convertase)	P29466	298	21	-45	18	
CaMK1δ	Pan-specific	Calcium/calmodulin-dep. protein-serine kinase 1 delta	Q8IU85	201	162	-46	10	
Hsc70	Pan-specific	Heat shock 70 kDa protein 8	P11142	297	32	-48	1	
Erk2	Pan-specific	Extracellular regulated protein kinase 2 (p42 MAPK)	P28482	507	42	-50	1	
JAK2	Pan-specific	Janus protein-tyrosine kinase 2	O60674	256	40	-52	1	
APG2	Pan-specific	Hsp 70-related heat shock protein 4 (HSP70RY)	P34932	376	65	-52	43	
Cyclin D1	Pan-specific	Cyclin D1 (PRAD1)	P24385	231	180	-55	35	
IKKα	Pan-specific	Inhibitor of NF-kappa-B protein kinase alpha (CHUK)	O15111	430	79	-58	12	
Bid	Pan-specific	BH3 interacting domain death agonist	P55957	430	65	-61	54	
Chk1	Pan-specific	Checkpoint protein-serine kinase 1	O14757	193	37	-73	9	

Target Protein Name	Phospho Site (Human)	Full Target Protein Name	Control (cpm)	+EGF (cpm)	%CFC	N
PED15 (PEA15)	S116	Phosphoprotein-enriched in diabetes/astrocytes 15	0	409	Increase	1
MRLC2	S18	Myosin regulatory light chain isoform 2	0	737	Increase	1
p38a MAPK	T180+Y182	Mitogen-activated protein kinase p38 alpha	0	398	Increase	3
EGFR	Y1148	Epidermal growth factor receptor kinase	0	2456	Increase	1
IRS1	Y1179	Insulin receptor substrate 1	0	1731	Increase	1
IRS1	Y612	Insulin receptor substrate 1	0	687	Increase	1
STAT1	Y701	Signal transducer and activator of transcription 1	0	1095	Increase	2
Hsp25	S86	Heat shock 25 kDa protein (mouse)	453	2671	489	1
Hsp27	S78	Heat shock 27 kDa protein beta 1 (HspB1)	706	3957	461	1
Fos	T232	Fos-c FBJ murine osteosarcoma transcr. factor	1054	4324	310	1
Erk1	T202+Y204	Extracellular regulated protein kinase 1 (p44 MAPK)	512	1466	186	5
Erk2	T185+Y187	Extracellular regulated protein kinase 2 (p42 MAPK)	521	1484	185	4
Shc1	Y349+Y350	SH2 domain-containing transforming protein 1	1082	2882	166	2
AcCoA Carb.	S80	Acetyl coenzyme A carboxylase	370	961	160	1
Rad17	S645	Rad17 homolog	4031	9310	131	1
GRK2	S670	G protein-coupled receptor kinase 2 (BARK1)	2058	4682	128	1
Raf1	S259	Raf1 proto-oncogene-encoded protein kinase	1573	3191	103	1
PDK1	S244	3-Phosphoinositide-dependent protein kinase 1	1470	2862	95	1
p53	S392	Tumor suppressor protein p53	811	1580	94	2
Jun	S73	Jun AP1 transcription factor p39	468	874	87	2
RSK1/2	S380/S386	Ribosomal S6 protein kinase 1/2	6632	12074	82	3
PKCβ1/2	T500	Protein kinase C beta 1/2	769	1377	79	1
Hsp27	S15	Heat shock 27 kDa protein beta 1 (HspB1)	1434	2558	78	1
Rb	S807	Retinoblastoma protein	4676	7436	59	2
PKCγ	T514	Protein kinase C gamma	1463	2296	57	1
FAK	S843	Focal adhesion protein kinase	415	645	55	2
PKCη	S674	Protein kinase C eta	707	1089	54	1
PKA Cβ	S338	cAMP-dep. protein kinase catalytic subunit beta	3747	5655	51	1
Hsp27	S82	Heat shock 27 kDa protein beta 1 (HspB1)	3593	5312	48	2
RSK1/2	S221/S227	Ribosomal S6 protein kinase 1/2	9332	13702	47	3
FAK	Y397	Focal adhesion protein kinase	1161	1650	42	1
NR1	S896	NMDA glutamate receptor 1 subunit zeta	1097	1544	41	1
Rb	S780	Retinoblastoma protein	7648	10658	39	1
GSK3β	Y216	Glycogen synthase kinase 3 beta p39	1387	1927	39	2
PKBα (Akt1)	S473	Protein kinase B alpha (Akt1)	1012	1366	35	3
eIF4E	S209	Euk. transl. Initiat. factor 4 (mRNA cap binding prot.)	764	1010	32	1
PKCγ	T655	Protein kinase C gamma	356	469	32	1
Rb	S807+S811	Retinoblastoma protein	5876	7720	31	1
MEK1	T385	MAPK/ERK protein kinase 1 (MKK1)	5937	7661	29	2
MLK3	T277+S281	Mixed-lineage protein-serine kinase 3	939	1180	26	1
PKCζ/λ	T410/T403	Protein kinase C zeta/lambda	1677	2068	23	1
IR	Y999	Insulin receptor	509	627	23	1
Erk5	T218+Y220	Extracellular regulated protein kinase 5 (BMK1)	403	482	20	1
MEK1/2	S217+S221	MAPK/ERK protein kinase 1/2 (MKK1/2)	1397	1593	14	1
ATF2	T51+T53	Activating transcription factor 2 (CRE-BP1)	3437	3794	10	2
Rb	T826	Retinoblastoma protein	4978	5478	10	2
Adducin α	S726	Adducin alpha (ADD1)	1443	1571	9	1
Bad	S75	Bcl2-antagonist of cell death protein	612	657	7	1
MEK1	T291	MAPK/ERK protein kinase 1 (MKK1)	8873	9414	7	2
MEK1	S297	MAPK/ERK protein kinase 1 (MKK1)	9231	9614	4	2
MARCKS	S158+S162	Myristoylated alanine-rich PKC substrate	1015	1039	2	1
RSK1/2	S363/S369	Ribosomal S6 protein kinase 1/2	13798	13898	1	3
JNK	T183+Y185	Jun N-terminus protein kinase (SAPK) p38	92	91	-1	4
Src	Y529	Src proto-oncogene-encoded protein kinase	1711	1675	-2	2
S6	S235	40S ribosomal protein S6	11237	10988	-2	1
Rb	S612	Retinoblastoma protein	933	908	-3	2
PKCδ	S664	Protein-serine kinase C delta	939	879	-6	1
Rb	T821	Retinoblastoma protein	2646	2420	-8	2
Vinculin	Y821	Vinculin	150	137	-8	1
PRAS40	T246	Proline-rich Akt substrate 40 kDa (Akt1S1)	5705	5124	-10	2
PTEN	S380+T382+S385	PIP3 3-phosphatase + tensin homolog	1041	928	-11	2
Paxillin 1	Y31	Paxillin 1	289	252	-13	1
Adducin γ	S693	Adducin gamma (ADD3)	1637	1431	-13	1
PKA Cα/β	T197	cAMP-dep. protein kinase cat. subunit alpha/beta	2033	1773	-13	1
mTOR	S2448	Mammalian target of rapamycin (FRAP)	422	364	-14	1
PKCα	S657	Protein kinase C alpha	4527	3827	-15	1
S6K2 p85	T444/S447	p85 ribosomal protein S6 kinase 2	1213	1017	-16	1
SOX9	S181	SRY (sex determining region Y)-box 9	1221	1019	-17	2
STAT3	S727	Signal transducer and activator of transcription 3	1815	1511	-17	2
PKCαβ2	T638/T641	Protein kinase C alpha/beta 2	400	331	-17	1

Target Protein Name	Phospho Site (Human)	Full Target Protein Name	Control (cpm)	+EGF (cpm)	%CFC	N
GSK3 α	Y279	Glycogen synthase kinase 3 alpha p44	1394	1123	-19	2
eIF4G	S1107	Eukaryotic transl. Initiat. factor 4 gamma 1	4851	3899	-20	2
Integrin β 1	S785	Integrin beta 1 (fibronectin receptor beta sub., CD29)	1785	1365	-24	1
Lyn	Y507	Yes-related protein kinase	3675	2804	-24	1
NMDAR2B	Y1474	(NMD) glutamate receptor 2B subunit	1289	972	-25	1
PKC γ	T674	Protein kinase C gamma	163	122	-25	1
Rb	T356	Retinoblastoma protein	6542	4674	-29	2
MEK2	T394	MAPK/ERK protein kinase 2 (MKK2) (human)	4562	3204	-30	2
CREB1	S133	cAMP response element binding protein 1	2607	1796	-31	1
CDK1/2	Y15	Cyclin-dependent protein kinase 1/2	11841	8150	-31	1
CDK1/2	T161/T160	Cyclin-dependent protein kinase 1/2	2982	2036	-32	1
PAK1/2/3	S144/S141/S154	p21-activated protein-serine kinase 1/2/3	10282	6858	-33	2
Dok2	Y142	Docking protein 2 (mouse)	6730	4449	-34	2
STAT1	S727	Signal transducer and activator of transcription 1	1731	1110	-36	1
ZAP70	Y292	Zeta-chain (TCR) associated protein kinase, 70 kDa	686	438	-36	1
Tau	S712	Microtubule-associated protein tau	1057	641	-39	1
GSK3 α	S21	Glycogen synthase kinase 3 alpha	757	455	-40	1
Pax2	S394	Paired box protein 2	1954	1151	-41	1
ErbB2	Y1248	ErbB2 (HER2, Neu) receptor-tyrosine kinase	370	218	-41	1
PRK2	T816	Protein kinase C-related protein-serine kinase 2	2126	1248	-41	1
eIF2 α	S51	Eukaryotic transl. Initiat. factor 2 alpha	2191	1233	-44	2
MAPKAPK2 α	T334	MAPK-activated protein kinase 2 alpha	2006	1121	-44	1
B23 (NPM)	T199	B23 (nucleophosmin, numatrin, NO38)	2501	1325	-47	1
FAK	S910	Focal adhesion protein kinase	1501	764	-49	2
FAK	Y576	Focal adhesion protein kinase	1029	523	-49	1
B23 (NPM)	T234+T237	B23 (nucleophosmin, numatrin, NO38)	4180	1954	-53	1
Cofilin 1	S3	Cofilin 1	7392	3434	-54	2
CDK1/2	T14+Y15	Cyclin-dependent protein kinase 1/2	9142	4017	-56	2
4E-BP1	S65	Euk. transl. Initiat. factor 4E binding prot. 1 (PHAS1)	186	81	-56	1
PRK1	T774	Protein kinase C-related protein-serine kinase 1	396	167	-58	1
B23 (NPM)	S4	B23 (nucleophosmin, numatrin, NO38)	5013	2058	-59	1
JNK	T183+Y185	Jun N-terminus protein kinase (SAPK) p46	109	45	-59	4
PKR	T451	Double-stranded RNA-dependent protein kinase	269	108	-60	2
S6K2 p85	T252	p85 ribosomal protein-serine S6 kinase 2	1071	390	-64	2
FAK	S722	Focal adhesion protein kinase	5104	1701	-67	2
Rac1/cdc42	S71	Ras-related C3 botulinum toxin substrate 1	3106	989	-69	2
Cortactin	Y470	Cortactin (amplaxin) (mouse)	1099	215	-80	2
PKC ϵ	S729	Protein kinase C epsilon	334	0	-100	1

Cell Line Name Tissue Source Cell Type	A431 Skin Epidermoid carcinoma	CaCo2 Colon Adeno- carcinoma	C2BBE1 Colon Adeno- carcinoma	CO Ovary Endo- metrial	COA3 Ovary Endo- metrial	ishikawa Ovary Adeno- carcinoma	HTR8 Ovary Tropho- blastoma	U87MG-EGFR Brain Glio- blastoma	
EGF Conc. (nM)	17	3	17	5	5	5	5	17	
Time (min)	10	10	10	5	5	5	5	10	
Number of Determinations	1 to 4	5	2	1	2	2	2	1	
Protein Name	Phospho-Site								
Erk2	T185+Y187	185	370	106	178	2450	77	8	-41
Erk1	T202+Y204	186	477	117	260	2100	81	-16	-45
MEK1/2	S217+S221	14	360	ND	-22	INCREASE	286	0*	-7
PKB α [Akt1]	S473	35	66	2	120	44	64	170	INCREASE
STAT3	S727	-17	131	ND	190	53	41	19	4
Raf1	S259	103	-17	ND	80	-45	148	-44	14
Rb	S807+S811	31	47	ND	0*	0*	0*	36	-6
p38 α MAPK	T180+Y182	INCREASE	-19	262	-46	-86	0	67	2
Adducin α	S726	9	43	ND	-6	-14	INCREASE	43	64
Rb	S780	39	62	ND	-52	0*	0*	56	-7
GSK3 β	S9	0	5	ND	47	0*	0*	0*	0*
Jun	S73	87	-15	ND	0*	0*	5	10	-1
PKC α/β	T638/T641	-17	56	ND	22	22	12	8	-25
NR1	S896	41	7	ND	ND	-10	47	-27	-6
PKC α	S657	-15	12	ND	116	14	-38	31	-60
JNK p46	T183+Y185	-59	115	-51	0*	0*	0	33	-26
GSK3 β	Y216	39	-42	ND	-26	0*	-8	6	34
GSK3 α	Y279	-19	21	ND	0*	-1	-21	-2	17
JNK p38	T183+Y185	-1	-29	47	0*	0*	-30	-12	13
CDK1/2	Y15	-31	ND	ND	-4	-46	26	-18	44
Src	Y529	-2	-9	-45	0*	8	-46	24	20
Adducin γ	S693	-13	-23	ND	-17	0*	0*	3	ND
Src	Y418	0	-41	-56	0*	0*	0*	0*	37
GSK3 α	S21	-40	-15	ND	0*	0*	0*	23	-40
PKR	T451	-60	-32	0*	0*	0*	0*	0*	34
CREB1	S133	-31	-75	ND	-36	-59	-14	-10	76
PKB α [Akt1]	T308	0	-50	ND	INCREASE	0*	-16	INCREASE	ND
PKC ϵ	S729	-100	-7	ND	0*	0*	-40	-18	49
CDK1/2	T14+Y15	-56	10	-53	ND	ND	ND	ND	ND
MEK2 human	T394	-30	ND	-45	ND	ND	ND	ND	ND
FAK	Y576	-49	ND	-51	ND	ND	ND	ND	ND
FAK	S722	-67	ND	-40	ND	ND	ND	ND	ND

Fig. 1

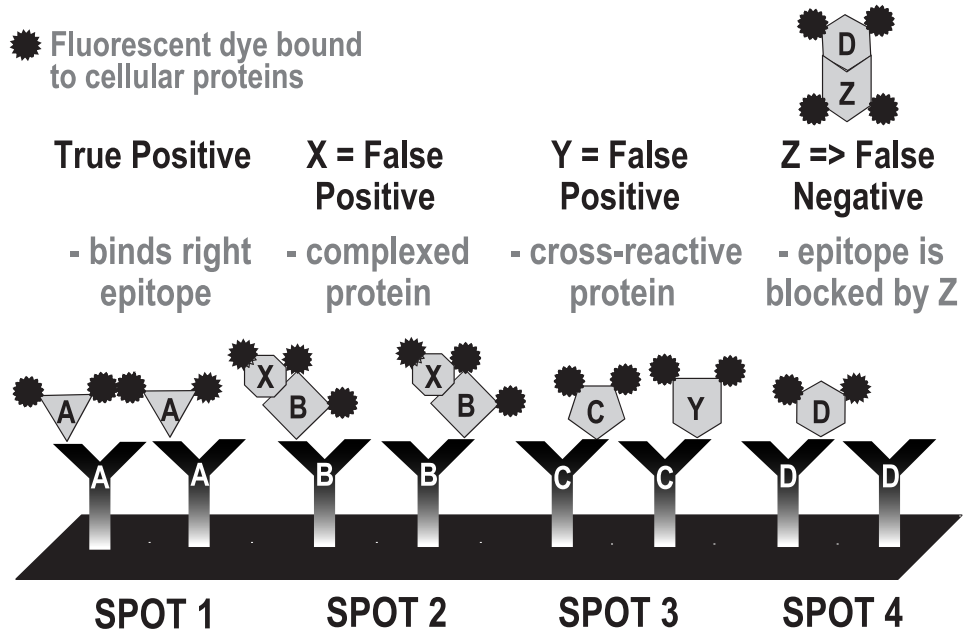


Fig. 2

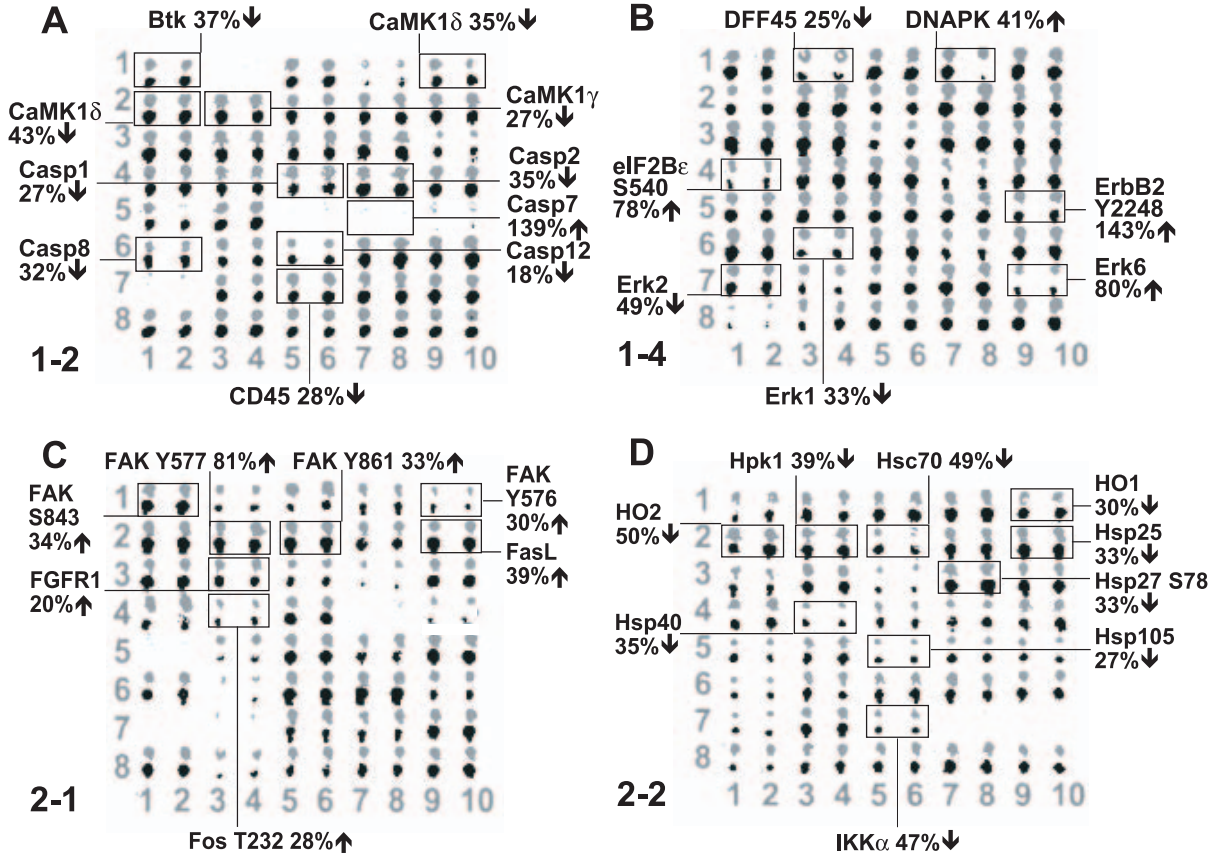


Fig. 3

